Light Emitting GaAs Nanowires on a Flexible Substrate

João Valente[1,†,], Tillmann Godde[2], Yunyan Zhang[1], David J. Mowbray[2] and Huiyun Liu[1]*

[1] Department of Electronic and Electrical Engineering, University College London, London WC1E 7JE, UK

[2] Department of Physics and Astronomy, University of Sheffield, Sheffield S3 7RH, UK

∗ Corresponding Author: joao.valente@glasgow.ac.uk \ †Present Address: Semiconductor Device Group, University of Glasgow, Glasgow G12

Semiconductor nanowire based devices are amongst the most promising structures to meet the current challenges of electronics, optics and photonics. Due to their high surface-volume ratio and excellent optical and electrical properties, low power, high efficiency and high-density devices can be achieved. This is of major importance for environmental issues and economic impact. Semiconductor nanowires have been used to fabricate high performance devices, including detectors, solar cells and transistors. Here we demonstrate a technique to transfer large area nanowire arrays to flexible substrates whilst retaining their excellent quantum efficiency in emission. Starting with a defect-free self-catalysed molecular beam epitaxy (MBE) sample grown on a Si substrate, GaAs core-shell nanowires are embedded in a dielectric, removed by reactive ion beam etching and transferred to a plastic substrate. The original structural and optical properties, including the vertical orientation, of the nanowires are retained in the final plastic substrate structure. Nanowire emission is observed for all stages

of the fabrication process, with a higher emission intensity observed for the final transferred structure, consistent with a reduction in non-radiative recombination via modification of surface states. This transfer process could form the first critical step in the development of flexible nanowire based light emitting devices.

KEYWORDS: Nanofabrication, Semiconductor Nanowires, Flexible Substrates, Photoluminescence.

Flexible electronic and photonic devices have been the focus of significant interest in the last few years. The flexibility of these devices allows the potential development of foldable and generally distortable sensors, detectors, circuits and photovoltaics[1–7]. Semiconductor nanowires, single crystals with diameters of a few nanometers and lengths on the micrometer scale, have already been used as fundamental building blocks in both electronic[8–12] and photonic[13–18] devices. A significant advantage of these structures is that they prevent the formation of some common defects, i.e. threading dislocations, hence reducing non-radiative phenomena and greatly improving device performance. In addition, their freestanding nature makes them ideal candidates for the basis of devices on flexible substrates. However, the structural composition and quality of the nanowires is critical for the optimised performance of the final devices. Semiconductor nanowires are usually grown on semiconductor substrates; this is a requirement for the control of defects and to achieve nanowires of the highest possible structural and optical quality[19–22]. The templates on which the nanowires are grown is hence of crucial importance to achieve high quality nanowires.

The ability to grow high quality semiconductor nanowires directly on flexible substrates is very restricted, due to a lack of suitable templates and the high temperatures needed for growth,

either by CVD or MBE; neither of these is compatible with direct growth on plastics[23, 24]. One exception is the fabrication of vertical ZnO nanowires directly on an indium-doped tin oxide (ITO) coated PET substrate[14], but this process is incompatible with the epitaxial techniques used to fabricated III-V nanowires. Given these difficulties an alternative approach is to form the nanowires on a semiconductor substrate and subsequently transfer them post-growth to a new and flexible substrate. Techniques to obtain nanowires on flexible substrates, based on mould or liquid transfer methods, have been widely reported. However, these generally result in horizontally oriented semiconductor nanowires on the flexible substrate[25–27]. For many applications, vertical oriented nanowires are required as this allows electrical contact to many nanowires in parallel, as required, for example, in edge emitting lasers[28] or where an array of nanowires is used to form components of a photonic crystal[29].

There have been a small number of reports of techniques which maintain the vertical orientation of the nanowires. These include an etching step which forms horizontal cracks in the nanowires, allowing them to be broken away from the substrate[30,31], a printing method[32], insertion into a PMMA [poly(methyl methacrylate)] layer[33] or embedding in a polydimethylsiloxane (PDMS) polymer matrix[34]. However, all these techniques were demonstrated for semiconductor nanowires with indirect bandgaps, Si in references [30, 31, 33 and 34] and GaP in reference [32], and hence no studies of the emissive properties of the transferred nanowires were possible. The transfer of nanowires retaining a high emission quantum efficiency is challenging, as any surface damage has a potential high impact in these large surface area to volume structures. For example, the etching steps of [30] and [31] may prove problematic, with the former also including a high temperature, high pressure step. Other techniques appear to require relatively long nanowires, [32], [33] and [34], and/or result in nanowires with a significant length distribution, [32] and [33], which complicates subsequent electrical contact. It is therefore necessary to develop a technique which allows the transfer of

large area arrays of vertical light emitting nanowires whilst preserving their initial high quantum efficiency.

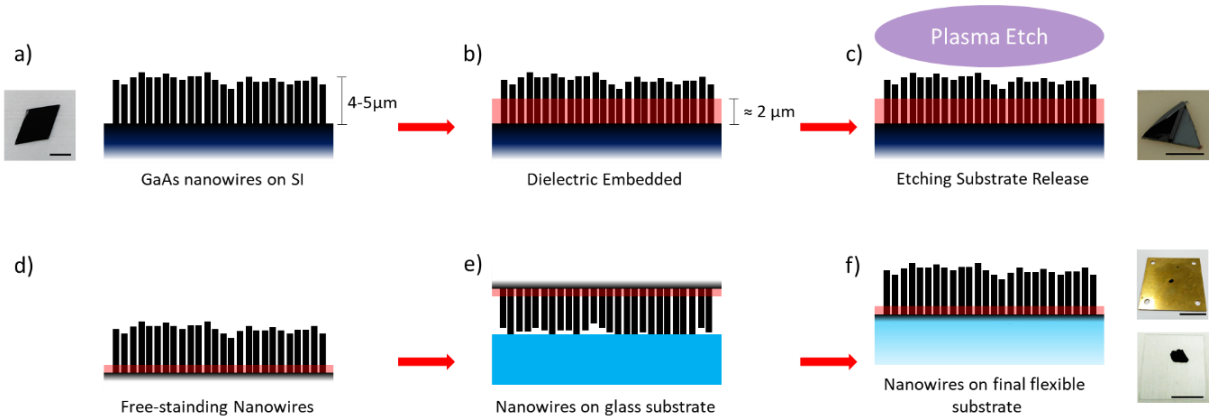

Figure 1: GaAs nanowires on flexible substrate fabrication process a) Molecular beam epitaxy as-grown GaAs nanowires on a silicon substrate. b) The same sample embedded with S01805 photoresist solution. c) Reactive ion etching with an SF_6 and O_2 plasma which releases the nanowires from the Si substrate. d) Free-standing nanowire layer that is transferable between substrates. e) GaAs nanowire free-standing layer initially transferred to an intermediate glass substrate. f) The nanowire layer transferred successfully to a flexible substrate. All the pictures show real samples at different stages of the growth and transfer process, the scale bars are 1cm.

In this paper, we report the fabrication of device-enabling, light emitting GaAs nanowires on flexible substrates (Figure 1) by contact transfer of a thin layer of nanowires. Following growth on a Si substrate (Figure 1a) and embedding within a dielectric (Figure 1b), a reactive ion etching step (Figure 1c) is introduced to release the nanowire layer from the substrate (Figure 1d). The nanowires are transferred to a new substrate via a liquid environment and an intermediate substrate (Figure 1e). The transferred layer preserves the nanowires' orientation and alignment, resulting in nanowires oriented perpendicular to the surface of the new substrate whilst retaining their emissive properties (Figure 1f). Compared to previous reports that also

used a dielectric layer[33,34], the present technique uses a more controlled reactive ion etching step rather than an applied force to remove the nanowires from the original substrate. The reactive ion etching step has a high degree of control and can be optimised to minimise damage to the nanowire surface whilst promoting detachment from the original Si substrate. The final transferred area varies from 1 mm^2 up to 1 cm^2, see pictures of the transferred samples in Figure 1f. By careful controlling the dielectric composition and/or reactive ion etching parametrization (gas fluxes, process time and RF power) and chemistry (gases used), it should be possible to extend this transfer technique to other III-V nanowire systems (i.e. InP, GaAsP, InGaAs etc.). Our results demonstrate the potential of this new transfer technique to develop high performance nanowire devices, for example solar cells, lasers and detectors, on flexible substrates.

Semiconductor nanowires were grown by MBE following a homogeneous core-shell architecture, with the same material, GaAs, deposited with different growth conditions for both the core and shell (see Methods). The growth conditions have been demonstrated to result in almost defect-free nanowire structures while allowing the subsequent growth of the shell material. The deposited nanowires are determined to have a length around 4-5 μm and a diameter of 200 nm, see Figure 2a. The surface of the nanowires is expected to form a thin oxide layer on exposure to the atmosphere. This layer will be present for all processing stages and the optical characterisations discussed below.

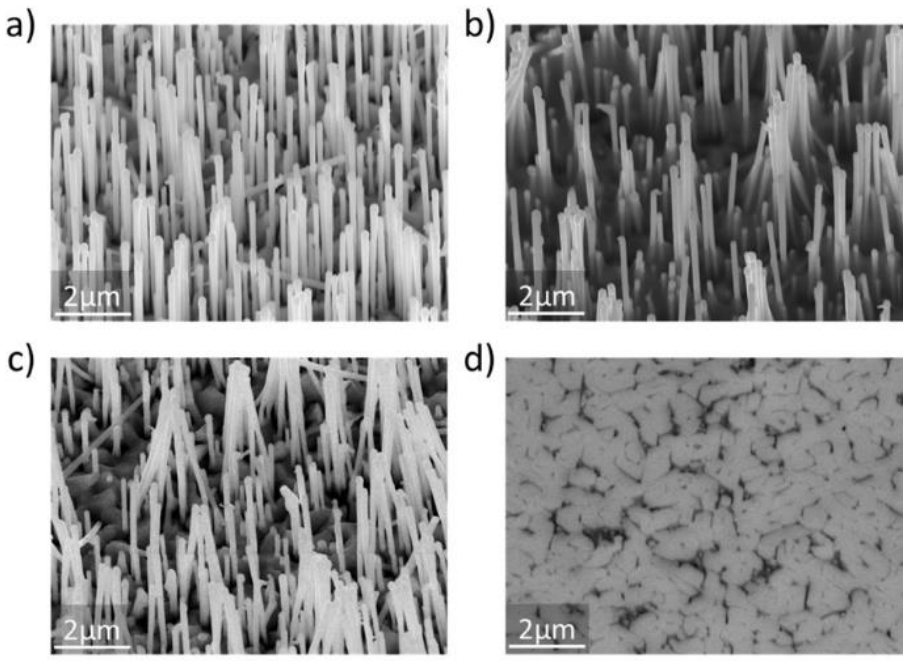

Figure 2: SEM image of GaAs nanowires at different processing stages. - SEM images of the GaAs nanowires during the different fabrication stages and on the final flexible substrate. a) As-grown GaAs nanowires on a silicon substrate. b) As-grown GaAs nanowires embedded within S1805 photoresist solution on the same substrate, prior to removal by reactive ion etching. c) SEM image of the transferred nanowire layer with the nanowire tips facing up. d) SEM image of the transferred nanowire layer with the cluster layer facing up.

The as-grown nanowires are not homogeneously spaced but are very straight and present homogeneous heights – Figure 2a. Additional material, referred to as clusters, is present on the substrate between the nanowires. It is believed that this is poly-crystalline GaAs and its deposition is associated with the growth conditions used to form nanowires on un-patterned substrates with a continuous oxide layer. Following growth, the nanowires were embedded within a dielectric layer by spin coating (see Methods). From several tested solutions, a 1:1 dilution of Photoresist S1805 with Ethylacetate was found to give the best coverage and impregnation following spinning and heat treatment. This solution has a low viscosity,

allowing for better flow in between the nanowires, while not being toxic and environmentally harmful, compared, for example, with BCB pastes. The as-grown nanowires on the silicon substrate are embedded within the dielectric photoresist by carefully spinning it into the nanowire sample and applying a heat treatment step. In order to dispense the photoresist solution without compromising the verticality of the nanowires and/or causing bending, a micro-pipette was used and the solution dispensed in a corner of the sample without nanowires present. In this way, the diluted photoresist solution is impregnated into the sample by capillary action along the surface and between the nanowires. Spinning the sample ensures a uniform thickness of the solution which is cured by the subsequent heat treatment. Overall, 4 dielectric layers are deposited to give a final thickness of around 2 μm, roughly half of the nanowire length. Depending on the dimensions of the grown nanowires, the dielectric layer thickness can be changed accordingly to achieve the correct dielectric to nanowire ratio (1:2).

Figure 2b shows a SEM image of the nanowires still on the Si substrate but embedded in the dielectric. It can be seen that there is a tendency for some nanowires to agglomerate together at their tips. Despite trying to minimize this phenomenon, the high nanowire density and their random spacing makes it impossible to totally eliminate this effect. Figure 2b clearly shows the presence of the dielectric and also that the cluster layer between the nanowires appears to be completely covered. Despite some islands of nanowires with their tips touching, the majority of the nanowires remain vertical and retain their original structural properties. The outcome of the processing steps is a nanowire layer which is sufficiently structurally robust to withstand the reactive ion etching process required to remove it from the Si substrate. This is achieved by impregnating a dielectric ‘glue’ layer within the nanowire ‘forest’.

Reactive ion etching (RIE) was used to release the nanowire-dielectric composite layer to give a substrate-free nanowire layer (see Methods). The sample was placed in the centre of the chamber and after the process is completed, the nanowire plus residual dielectric composite

layer curls upon itself, sitting on the silicon substrate (see picture on Figure 1c). The detached free-standing layer is now transferrable to a new host substrate. In the current study, this newly 'peeled-off' nanowire layer was transferred to a plastic substrate via liquid immersion in methanol.

SEM images of a nanowire layer transferred onto a plastic substrate is shown in Figures 2c and d. Figure 2c shows the layer with the desired orientation, with the nanowire tips away from the substrate and facing the electron beam. Figure 2d shows the nanowires bases / clusters facing the electron beam, representing the intermediate stage of the transfer process (Figure 1e). It is interesting to note that the image from the nanowire side shows little evidence of the dielectric layer between the nanowires, except a thin layer over the previously observable clusters. This indicates that the reactive ion etching process also affects the dielectric layer, decreasing its thickness although not removing it completely. For the purpose of this work the presence of the dielectric after the etching process is not relevant; as shown below the optical and structural properties of the transferred nanowires do not appear to be significantly affected by the dielectric. Any subsequent electrical contacting would most likely require the region between the nanowires to be completely infilled with an insulating material to provide a planar surface for the top electrical contact. This could be achieved by adding additional photoresist layers. The image taken from the cluster side (Figure 2d) indicates a very homogeneous and compact layer which makes the entire layer structurally stable, aiding the successful transfer of the nanowires to the new plastic substrate. For every transferred sample the adhesion to the new substrate after drying of the methanol was observed to be very strong. Water and IPA rinsing did not affect nanowires placement and even after physical abrasion of the surface remains of the cluster layer could be observed.

Following the successfully transfer of vertically oriented GaAs nanowires onto a flexible substrate, the structural and optical properties were studied and compared to those of the as-

grown nanowires still attached to a silicon substrate. Raman spectroscopy was applied to probe the structural composition by determining the frequencies of the optical phonons. These depend upon the material composition but can also be affected by strain. Raman spectra were measured over the range 200 cm^{-1} to 600 cm^{-1}, see Methods for further details. Despite the diameter of each nanowire being around 200 nm, roughly 2 to 5 nanowires are probed when considering the nanowire areal density ($1.8x10^8$ cm^{-2}). When embedded in the dielectric the number may increase because of the tendency for the tips to agglomerate. In zinc-blende GaAs the room temperature zone centre TO and LO phonon frequencies are 267 cm^{-1} and 291 cm^{-1} respectively. The as-grown semiconductor nanowires (green curve) show the LO and TO modes of GaAs on a very flat background, characteristic of a crystalline substrate, such as silicon. For the as-grown sample, the TO and LO phonons are shifted slightly to 266 cm^{-1} and 289 cm^{-1} respectively. This shift is attributed to strain in the nanowires.

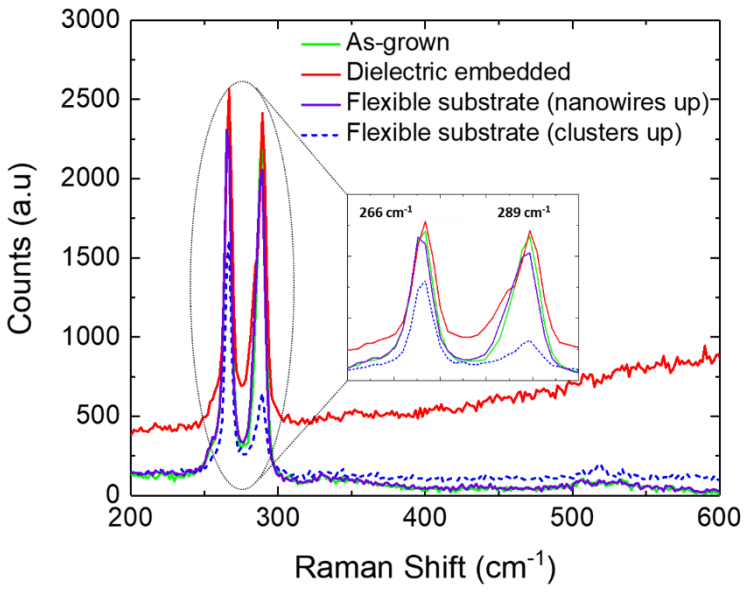

Figure 3: Raman spectra of GaAs nanowires on a flexible substrate - Raman spectra of as-grown semiconductor nanowires (green curve), embedded sample (red curve) and nanowires on a plastic substrate with the nanowires (purple curve) or the clusters (dashed blue curve)

facing the laser. The Brillouin-zone centre GaAs TO and LO phonon frequencies at room temperature are 267 cm^{-1} and 291 cm^{-1} respectively.

The red spectrum in Figure 3 is for the dielectric embedded nanowires still attached to the silicon substrate. The main change is the presence of a broad background due to the dielectric, see Supplementary Information (Fig S2). The relative intensities, frequencies and linewidths of the TO and LO phonons are identical to those of the as-grown structure. This confirms that despite the embedding of the nanowires within the dielectric followed by heat treatment, their composition is not significantly altered. The temperature used for the heat treatment is significantly less than the growth temperature and so is not expected to result in structural changes, the Raman spectra confirm this. The purple and dashed blue line spectra are for measurements preformed on nanowires transferred to the plastic substrate, with the nanowires (purple) or the clusters (dashed blue) facing the laser. The nanowires facing the laser have TO and LO phonon modes at identical frequencies to the as-grown sample and exhibit the same relative intensity. When the clusters face the laser, the same two modes are present but there is a large reduction in the relative intensity of the LO phonon. As the selection rules for scattering by LO or TO phonons depends on the surface orientation, the change in the relative LO:TO intensity is consistent with scattering from a randomly oriented polycrystalline matrix. Our results hence indicate that the clusters are polycrystalline with different crystal orientations facing the laser, and poor crystal quality when compared with the nanowires. The Raman spectra of the transferred sample with the clusters facing the laser also exhibits a very weak feature at 519 cm^{-1}, corresponding to the optical phonon frequency of bulk Si. The presence of this feature indicates that a small amount of Si from the substrate is included in the transfer process, likely to arise from the reactive ion etching interface (silicon substrate and GaAs cluster layer). It is not possible to estimate the amount of Si transferred but given that the

corresponding Raman feature is much weaker than that of the GaAs phonons and also that Si is a relatively strong Raman scatterer, the amount of transferred Si is very small. The present Raman measurements demonstrate that nanowires transferred to plastic substrates exhibit identical optical phonon characteristics as the as-grown and dielectric embedded on silicon samples. There is a clear difference in the spectra recorded from the transferred samples with either the nanowire tips or bases towards the laser. This difference is attributed to the presence of polycrystalline GaAs clusters which are also transferred from the silicon substrate.

Whilst Raman analysis provides important information on the structural properties of the samples it is also desirable to directly probe their electronic structure. This was achieved by performing micro photoluminescence (μPL) which probes an area ~1 μm^2. More details on the μPL measurement setup can be found in Methods. As is the case for the Raman measurements, it is estimated that approximately 2 to 5 nanowires are probed in the as-grown sample. For the dielectric embedded and structure transferred to the flexible substrate the tendency for tips of neighbouring nanowires to agglomerate may result in a larger number of nanowires being probed. The laser was focussed at the tips of the nanowires which enhances their signal with respect to the cluster emission. The nanowires and clusters are found to emit light at different wavelengths allowing their relative contributions to be spectrally resolved. As both nanowires and clusters are inhomogeneously distributed on a micrometer scale, as observable in Figure 2, the μPL is also spatially inhomogeneous. Hence initial characterisation of the samples involved a spatial mapping, constructed from individual μPL spectra recorded for a spatial step size of 0.5 μm over an area between 35x35 and 70x70 μm^2. Example maps and spectra are shown in the Supplementary Information (Figures S3 and S4). From this mapping it is possible to identify regions with either a strong nanowire or cluster emission for each stage of fabrication steps (referred to as nanowire or cluster rich regions, see Figure S5) which could then be studied in more detail.

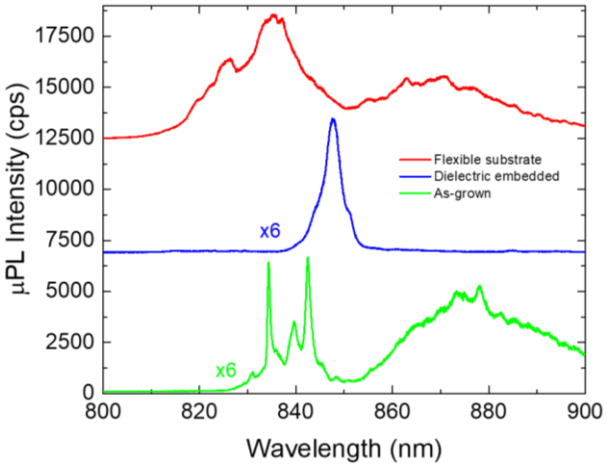

Figure 4: Comparison μPL spectra. Photoluminescence spectra from nanowire rich regions for the three stages of the growth and transfer process. Vertical offsets have been applied to the spectra of the dielectric embedded and flexible substrate structures for clarity. The laser power is ~ 0.6 μW.

Figure 4 shows typical PL spectra recorded from a NW rich region for the three stages of the growth and transfer process. The longer wavelength ($\gtrsim$ 845 nm), broad emission is attributed to the clusters and the sharper, shorter wavelength emission to the nanowires. Even in nanowire rich regions strong cluster emission is present, with the exception of the dielectric embedded sample. For all three samples the nanowire emission occurs predominantly below the low temperature bandgap of GaAs (1.51 eV ≡ 820 nm for the Zinc Blende structure). Given the size of the nanowires (diameter 200 nm), confinement energies are expected to be very small (estimated from an infinite potential well model to be less than 1 meV). A similar below bandgap emission has been reported in other studies of GaAs nanowires[35-37]. The exact reason for this below bandgap emission remains unclear although in [37] it was attributed to type-II indirect real space recombination between electrons spatially localised in Zinc Blende regions of the wire and holes spatially localised in Wurzite regions. Previous structural studies[21] of similar nanowires to those studied here suggest a predominantly Zinc Blende structure. Any

Wurzite regions are expected to be very small and concentrated towards the edges of the wires, these regions are therefore not expected to have a significant influence on the optical properties.

The spectrum of the as-grown structure shows a number of sharp lines (approximately 5 are visible) in the region ~830-850 nm. These lines could arise either from different nanowires or from localised states (bulk or surface) in the same nanowire. Given that their number correlates with the number of nanowires expected to be probed by the experimental geometry they are attributed to emission by individual nanowires. Line widths as small as 0.6nm (≡ 1.0meV) are measured.

The emission from the dielectric embedded and flexible substrate structure is shifted with respect to the as-grown structure, to longer wavelengths for the former and shorter wavelengths for the latter. This appears to be a common trend when studying different spatial positions across the surface, as shown in Figure S6. Both the emission from the dielectric embedded and flexible substrate sample show a substructure but with lines that are much less well defined in comparison to the as-grown structure. Further information is provided by power dependent μPL studies which are discussed below.

To further study the emission properties of the nanowires, power dependent μPL spectra were recorded for excitation powers over the range 50nW to 100μW. Figures 5a, b and c show representative spectra for the three stages of the transfer process, in each case the spectra are recorded from a nanowire rich region.

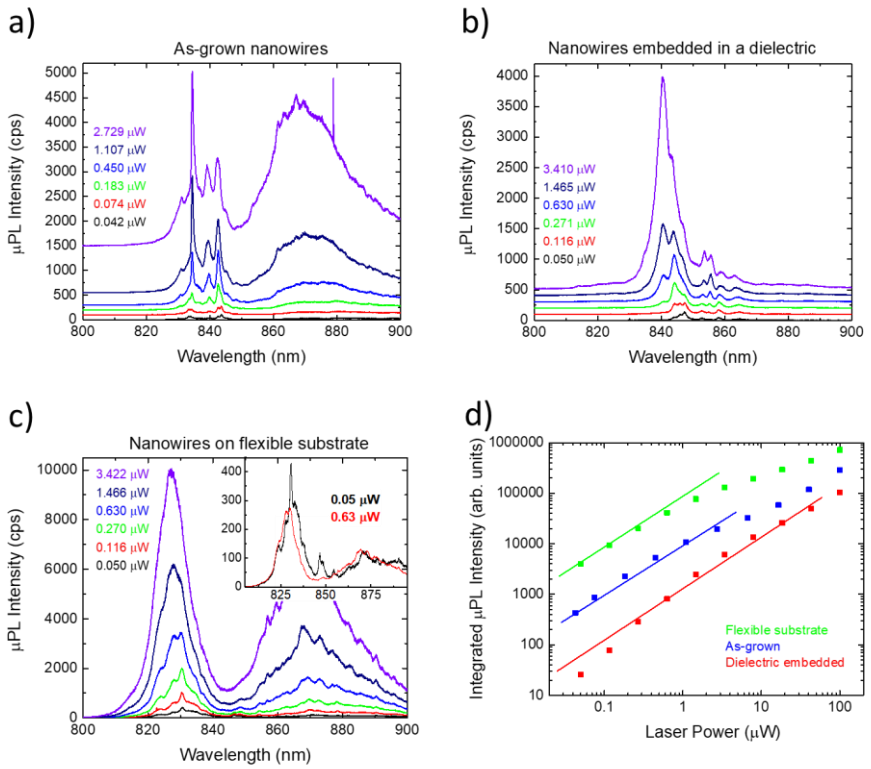

Figure 5: μPL power dependency study. μPL measurements for different laser powers (0.04 μW - 3.4 μW) from different steps of the fabrication process. a) As-grown nanowires sample. b) Dielectric embedded nanowire sample. c) Nanowires on the flexible substrate sample. The inset to c) compares PL spectra for two different powers, normalised to the laser power. The spectra in a) and b) are offset vertically for clarity. d) Integrated nanowire emission (for the spectral range 800 to 840 nm) for the three steps of the fabrication process. The solids lines are guides to the eye and have unity gradient, consistent with excitonic recombination. All the data in this figure is recorded from nanowire rich regions of the three structures.

A small blue shift of the emission, typically ~0.5meV, is observed when the laser power is increased by ~10^3. Such a blue shift is expected for a spatially indirect type-II transition with electrons and holes separately localised in Zinc Blende and Wurzite structure regions of the nanowire. The very small blue shift observed indicates that this is a very small effect in the current structures. In addition, the line width of the sharp sub-features increases with laser

power, typically doubling when the laser power is increased by ~10^3. This behaviour is shown in the inset to Figure 5c, which compares spectra at two powers differing by a factor of 13 for the flexible substrate structure. Hence the different forms of the spectra for the three structures at a common power (Figure 5d) appear to result from the power dependence of the emission linewidths.

Figure 5d shows the power dependence of the nanowire emission intensity for the three structures. Because of the complex nature of the emission, the nanowire emission intensity was obtained by integrating the relevant spectra over the range 800 to 840 nm. At low powers, the emission of all three structures increases approximately linearly with power, suggesting a predominantly excitonic recombination. At high powers, the power dependence of the emission becomes sub-linear, consistent with a saturation behaviour. The departure from a linear behaviour occurs at progressively lower powers for the dielectric embedded, as-grown and flexible substrate structure respectively. This trend, coupled with the higher emission intensity in the progression dielectric embedded, as-grown and flexible substrate structure respectively, is consistent with an increase in the carrier density at a given laser power through this sample progression. A higher carrier density in the flexible substrate structure is also consistent with lower laser powers being required to observe the sharp nanowire emission. A variation in carrier density for a constant laser power requires the carrier lifetime to vary between structures. The most likely candidate for this is a variation in the non-radiative lifetime, possibly as a result of modifications to the nanowire surfaces.

The results of Figures 3, 4 and 5 demonstrate that structural properties with strong nanowire emission is retained following transfer from the Si substrate to a flexible substrate, although there are some changes to the detailed properties of this emission. Therefore, as-grown nanowires can be embedded within a dielectric layer without a deterioration of the structural and optical properties. A composite ‘free-standing’, transferable nanowire layer is produced

after reactive ion etching removes it from the original Si substrate. This process increases the versatility of the nanowires, since they can now be transferred to different non-semiconductor substrates, opening up a range of applications. These nanowire free-standing layers have been successfully transferred to plastic, glass and copper substrates, whilst preserving the structural and optical properties. It should be possible to increase the yield of the transfer process by introducing an extra drying step, for example CO_2 critical-point drying[38,39]. This newly developed flexible nanowire platform could form the basis for foldable and generally distortable nanowires sensors, detectors, circuits and photovoltaics. Such devices can provide higher efficiencies, improved performance and lower environmental impact. By transferring a dielectric embedded nanowire layer to a transparent conductive oxide (TCO) coated flexible substrate, followed by the deposition of a top contact, a flexible nanowire solar cell can be envisioned. As part of the current studies we have shown that the nanowires can be transferred to a number of different surfaces, including plastic, metal and glass, with excellent adhesive properties. Electrical addressing of a flexible layer through conductive clusters could allow electrical excitation of the luminescence. Finally, this transferrable large area nanowire free-standing layer can be combined with metamaterials and quantum systems to study new physics.

In summary, optically active flexible nanowire structures have been achieved by initial growth on Si substrates, followed by transfer to a plastic substrate. The transfer process retains the nanowire structural and optical properties. Nanowire emission is observed at all stages of the fabrication process, with evidence to suggest reduced non-radiative recombination in the transferred nanowires, possibly due to modification of surface states. The demonstration of optically active nanowires on a plastic substrate is an important first step in the fabrication of flexible electronic or optoelectronic devices. Possible devices include flexible nanowire solar cells or complex circuits incorporating transistors and/or lasers.

METHODS

Nanowire Growth

Gallium droplet catalysed nanowires were grown on native-oxide-covered p-type Si (111) substrates by solid-source III-V MBE. The GaAs nanowire cores were grown with a Ga beam equivalent pressure, V/III flux ratio, substrate temperature, and growth duration of 8.41×10^{-8} Torr, 44, ≈630ºC, and 1 hour, respectively. After the core-nanowire growth, the Ga-droplets are consumed by closing the Ga flux but keeping open the As flux. The GaAs shell was grown with the same Ga beam equivalent pressure and time as for the core, while the V/III flux ratio and substrate temperature were changed to 50 and ≈340 ºC, respectively. The substrate temperature was measured by a pyrometer.

Dielectric embedding of nanowires

A dielectric solution of photoresist S1805 diluted in Ethylacetate, ratio 1:1, was spun on the as-grown GaAs nanowires sample in order to impregnate dielectric into the nanowire forest. The spin coating consists of 3 steps: initial spinning at 500 rpm for 2 seconds, 1000 rpm for 10 seconds and finally 3000 rpm for 30 seconds. This multistep spinning results in a thinner dielectric layer with increased homogeneity. In addition, by slowly increasing the rotation speed, bending and damage of the nanowires is minimized. All speed increases occur with a ramp-up of 2 seconds. Heat treatment between each of the 4 layers consists of a 60 second bake at 115 ºC. After the spin steps, the sample is developed in MF26 solution for 90 seconds. A hard bake is applied for 2 minutes at 115 ºC. All heat treatments are performed in a cleanroom environment using a hot plate.

Reactive Ion Etching and Nanowire layer transfer

The nanowires embedded in the dielectric matrix were placed inside a reactive ion etching system (Oxford Plasma Pro NGP 80 RIE) and etched in SF_6 (12 sccm) and O_2 (3 sccm) for 15 minutes. The base pressure was 5.5×10^{-6} mTorr and power 200 W. When the chamber is opened following the RIE process the nanowire layer is seen to be curled upon itself and remains on the silicon substrate, see Figure 1c and d. The last step to achieve nanowires on flexible substrates is to transfer this newly peeled off nanowire layer on to a plastic substrate through liquid immersion in Methanol. First, a temporary glass substrate was placed on top of the curled layer. When this substrate approaches the dielectric embedded nanowire layer, the layer uncurls, allowing the temporary substrate to be placed on top of the nanowires (Figure 1e). At this point the nanowires are transferred, with the cluster side facing outwards, to the glass substrate in the presence of methanol. In order to invert the orientation of the nanowires, a repetition of the transfer process is applied, but with a final plastic substrate, Figure 1f. Air drying was applied to remove the methanol.

Raman

Raman spectra are measured using a Renishaw RE04 system with a 532nm CW diode laser, incident perpendicular to the sample. The laser power is approximately 0.5mW and the spot size (obtained with a 50x objective lens) has a working depth of 370 μm and a diameter of 1 μm. Spectra are obtained from 200 cm^{-1} to 600 cm^{-1} and averaged for 3 accumulations.

Micro Photoluminescence (μPL)

μPL spectra were measured with a 515 nm excitation laser, 1 s integration time and with the sample in a high vacuum inside a flow cryostat (base temperature 6 K). The incident laser was focused with an Olympus 20x long working distance microscope objective to a spot size of 1 μm diameter. The resultant PL was collected by the same microscope objective and focused into a 0.75 m spectrometer, where the spectral components were resolved and detected using a 600 l/mm grating and a nitrogen cooled CCD. The spectral resolution was 0.2 meV.

References

[1] Chen, Y., Li, H., & Li, M. (2012). Flexible and tunable silicon photonic circuits on plastic substrates. Scientific Reports, 2, 622. https://doi.org/10.1038/srep00622

[2] Walia, S., Shah, C. M., Gutruf, P., *et al.* (2015). Flexible metasurfaces and metamaterials: A review of materials and fabrication processes at micro- and nano-scales. Applied Physics Reviews, 2(1). https://doi.org/10.1063/1.4913751

[3] Pu, J., Yomogida, Y., Liu, K. K., Li, L. J., Iwasa, Y., & Takenobu, T. (2012). Highly flexible MoS 2 thin-film transistors with ion gel dielectrics. Nano Letters, 12(8), 4013–4017. https://doi.org/10.1021/nl301335q.

[4] Hu, P., Wang, L., *et al.* (2013). Highly responsive ultrathin GaS nanosheet photodetectors on rigid and flexible substrates. Nano Letters, 13(4), 1649–1654. https://doi.org/10.1021/nl400107k

[5] Koo, M., Park, K. *et al.* (2012). Bendable inorganic thin-film battery for fully flexible electronic systems. Nano Letters, 12(9), 4810–4816. https://doi.org/10.1021/nl302254v

[6] Liu, N., Tian, H., Schwartz, G., Tok, J. B. H., Ren, T. L., & Bao, Z. (2014). Large-area, transparent, and flexible infrared photodetector fabricated using P-N junctions formed by N-doping chemical vapor deposition grown graphene. Nano Letters, 14(7), 3702–3708. https://doi.org/10.1021/nl500443j

[7] Hyun, W. J., Park, O. O., & Chin, B. D. (2013). Foldable graphene electronic circuits based on paper substrates. Advanced Materials, 25(34), 4729–4734. https://doi.org/10.1002/adma.201302063

[8] Aberg, I., Vescovi, G., *et al.*. (2016). A GaAs nanowire array solar cell with 15.3% efficiency at 1 sun. IEEE Journal of Photovoltaics, 6(1), 185–190. https://doi.org/10.1109/JPHOTOV.2015.2484967

[9] Huihui, Y., Rui, J., Chen, C., Misra, S., Yu, L., Chen, W., & InGaP-on-Si, S. (2015). InGaAs axial-junction nanowire-array solar cells. J. Appl. Phys, 54.

[10] Dorodnyy, A., Alarcon-Lladó, E., Shklover, V., Hafner, C., Fontcuberta I Morral, A., & Leuthold, J. (2015). Efficient Multiterminal Spectrum Splitting via a Nanowire Array Solar Cell. ACS Photonics, 2(9), 1284–1288. https://doi.org/10.1021/acsphotonics.5b00222

[11] M. Yao, N. Huang, S. Cong, *et al.*, GaAs Nanowire Array Solar Cells with Axial p−i−n Junctions, Nano Letters, 14, 3293 (2014), ISSN 15306992.

[12] Wu, J., Li, Y., Kubota, J., *et al.* (2014). Wafer-scale fabrication of self-catalyzed 1.7 eV GaAsP core-shell nanowire photocathode on silicon substrates. Nano Letters, 14(4), 2013–2018. https://doi.org/10.1021/nl500170m

[13] Duan, X., Niu, C., Sahi, V., *et al.* (2003). High-performance thin-film transistors using semiconductor nanowires and nanoribbons. Nature, 425(6955), 274–278. https://doi.org/10.1038/nature01996

[14] Zeng, Y., Pan, X., Lu, B., & Ye, Z. (2016). Advances Fabrication of flexible self-powered UV detectors based on ZnO nanowires and the enhancement by the decoration of Ag nanoparticles. RSC Advances, 6, 31316–31322. https://doi.org/10.1039/C6RA02922A

[15] Couteau, C., Larrue, A., Wilhelm, C., & Soci, C. (2015). Nanowire Lasers. Nanophotonics, 4(1), 90–107. https://doi.org/10.1515/nanoph-2015-0005

[16] Li, K. H., Liu, X., Wang, Q., Zhao, S., & Mi, Z. (2015). Ultralow-threshold electrically injected AlGaN nanowire ultraviolet lasers on Si operating at low temperature. Nature Nanotechnology, 10(2), 140–4. https://doi.org/10.1038/nnano.2014.308

[17] Zhu, H., Fu, Y., Meng, F., *et al.* (2015). Lead halide perovskite nanowire lasers with low lasing thresholds and high-quality factors. Nature Materials, 14(6), 636–642. https://doi.org/10.1038/nmat4271

[18] Cao, L., & Brongersma, M. L. (2009). Engineering light absorption in semiconductor nanowire devices. Nature Materials, 8(8), 643–7. https://doi.org/10.1038/nmat2477

[19] Tatebayashi, J., Kako, S., Ho, J., Ota, Y., Iwamoto, S., & Arakawa, Y. (2015). Room-temperature lasing in a single nanowire with quantum dots. Nature Photonics, advance on (8), 1–16. https://doi.org/10.1038/nphoton.2015.111

[20] Wu, J., Ramsay, A., Sanchez, A., *et al.* (2016). Defect-Free Self-Catalyzed GaAs/GaAsP Nanowire Quantum Dots Grown on Silicon Substrate. Nano Letters, 16(1), 504–511. https://doi.org/10.1021/acs.nanolett.5b04142

[21] Zhang, Y., Fonseka, H. A., Aagesen, M., *et al.* (2017). Growth of Pure Zinc-Blende GaAs(P) Core–Shell Nanowires with Highly Regular Morphology. Nano Letters, acs.nanolett.7b02063 https://doi.org/10.1021/acs.nanolett.7b02063

[22] Sourribes, M. J. L., Isakov, I., Pan, M., Liu, H., & Warburton, P. A. (2014). Mobility Enhancement by Sb-mediated Minimisation of Stacking Fault Density in InAs Nanowires Grown on Silicon. Nano Letters, 14.

[23] Zhang, Y., Wu, J., Aagesen, M., Holm, J., *et al.* (2014). Self-catalyzed ternary core-shell gaasp nanowire arrays grown on patterned Si substrates by molecular beam epitaxy. Nano Letters, 14(8), 4542–4547. https://doi.org/10.1021/nl501565b

[24] Goto, H., Nosaki, K., Tomioka, K., *et al.* (2009). Growth of core-shell InP nanowires for photovoltaic application by selective-area metal organic vapor phase epitaxy. Applied Physics Express, 2(3). https://doi.org/10.1143/APEX.2.035004

[25] Liu, X., Long, Y., Liao, L., Duan, X., & Fan, Z. (2012). Large-Scale Integration of Semiconductor Nanowires for High-Performance Flexible Electronics. ACS Nano, 6(3), 1888–1900. https://doi.org/10.1021/nn204848r

[26] Smith, D. A., Holmberg, V. C., & Korgel, B. A. (2010). Flexible Germanium Nanowires: Ideal Strength, Room Temperature Plasticity, and Bendable Semiconductor Fabric. ACS Nano, 4(4), 2356–2362.

[27] Mcalpine, M. C., Ahmad, H., Wang, D., & Heath, J. R. (2013). Highly ordered nanowire arrays on plastic substrates for ultrasensitive flexible chemical sensors. Nature Materials, 6(5), 379–384. https://doi.org/10.1038/nmat1891

[28] Thomas Frost, Shafat Jahangir, Ethan Stark, Saniya Deshpande, Arnab Hazari, Chao Zhao, Boon S. Ooi, and Pallab Bhattacharya. Monolithic Electrically Injected Nanowire Array Edge-Emitting Laser on (001) Silicon, Nano Lett. 2014, 14, 4535−4541, dx.doi.org/10.1021/nl5015603 |

[29] Yuerui Lu and Amit Lal, High-Efficiency Ordered Silicon Nano-Conical-Frustum Array Solar Cells by Self-Powered Parallel Electron Lithography, Nano Lett. 2010, 10, 4651–4656, DOI: 10.1021/nl102867a

[30] Jeffrey M. Weisse, Dong Rip Kim, Chi Hwan Lee, and Xiaolin Zheng, [Vertical Transfer of Uniform Silicon Nanowire Arrays via Crack Formation, Nano Lett. 2011, 11, 1300–1305, dx.doi.org/10.1021/nl104362e

[31] Han-Jung Kim, Jihye Lee, Sang Eon Lee, Wanjung Kim, Hwan Jin Kim, Dae-Geun Choi, and Jong Hyeok Park, Polymer-free Vertical Transfer of Silicon Nanowires and their Application to Energy Storage, ChemSusChem 2013, 6, 2144 – 2148

[32] Inga von Ahnen Gaëlle Piret Christelle N. Prinz, Transfer of vertical nanowire arrays on polycaprolactone substrates for biological applications, Microelectronic Engineering 135 (2015) 52–56, dx.doi.org/10.1016/j.mee.2015.03.007

[33] Shu-Chia Shiu, Shih-Che Hung, Jiun-Jie Chao, Ching-Fuh Lin, Massive transfer of vertically aligned Si nanowire array onto alien substrates and their characteristics, Applied Surface Science 255 (2009) 8566–8570

[34] Katherine E. Plass, Michael A. Filler, *et al.* (2009). Flexible Polymer-Embedded Si Wire Arrays. Advanced Materials, 21, 325–328. https://doi.org/10.1002/adma.200802006

[35] Gustafsson, A., Bolinsson, J., Ek, M., & Samuelson, L. (2011). GaAs-based Nanowires Studied by Low-Temperature Cathodoluminescence. Journal of Physics: Conference Series, 326, 12042. https://doi.org/10.1088/1742-6596/326/1/012042

[36] Bolinsson, J., Ek, M., Trägårdh, J *et al.* (2014). GaAs/AlGaAs heterostructure nanowires studied by cathodoluminescence. Nano Research,7(4), 1–18. https://doi.org/10.1007/s12274-014-0414-2

[37] Couto, O. D. D., Sercombe, D., Puebla, J., *et al.* (2012). Effect of a GaAsP shell on the optical properties of self-catalyzed GaAs nanowires grown on silicon. *Nano Letters*, *12*(10), 5269–5274. https://doi.org/10.1021/nl302490y

[38] Ijaz H. Jafri, Heinz Busta, Steven T. Walsh, (1999) Critical point drying and cleaning for MEMS technology. *Proc. SPIE , MEMS Reliability for Critical and Space Applications*, (*3880*). https://doi.org/10.1117/12.359371

[39] Keiichi Tanaka and Akihiro Iino (1974) Critical Point Drying Method Using Dry Ice. *Stain Technology Vol.* 49(4). https://doi.org/10.3109/10520297409116978

Author contribution: The idea of the work was conceived by J.V and H.L.; Y.Z. was responsible for the nanowires growth; T.G carried out the μPL measurements; all authors discussed the results and analysed the data; J.V., T.G. and D. J. M. wrote the paper; H.L. supervised the work.

Supporting Information: Comparison of Raman spectra with and without dielectric layer on the GaAs nanowires. Typical spectra from Nanowire rich areas. Micro-Photoluminescence colour maps. Comparison spectra between cluster rich and nanowire rich areas for the 3 different steps of fabrication process. Micro-photoluminescence results for different nanowire rich areas for the 3 different steps of fabrication process, spatial variability.

Acknowledgements: The authors acknowledge the support of Leverhulme Trust and the U.K. Engineering and Physical Sciences Research Council - EPSRC (grant nos. EP/P000916/1 and EP/P000886/1).

Additional information: Competing financial interests: The authors declare no competing financial interests.